On the observed connection between Arctic sea ice and Eurasian snow in relation to the winter NAO

Author: MARÍA SANTOLARIA OTÍN

Supervisors:
JOAN BECH, joan.bech@ub.edu
Facultat de Física, Universitat de Barcelona, Martí i Franquès 1, 08028 Barcelona, Spain.*

JAVIER GARCÍA SERRANO, javier.garcia@bsc.es; MARTIN MÉNÉGOZ, martin.menegoz@bsc.es.
Earth Sciences Dept., Barcelona Supercomputing Center (BSC-CNS), Barcelona, Spain.

Abstract: Many recent studies reveal that sea ice concentration (SIC) in the eastern Arctic and snow cover extent (SCE) over central Eurasia in late autumn are potential predictors of the winter North Atlantic Oscillation (NAO). We used maximum covariance analysis (MCA) to investigate the links between autumn SIC in the Barents-Kara Seas (BK) and SCE over Eurasia (EUR) with winter (DJF) sea level pressure in the North-Atlantic-European region over 1979-2015. The most significant covariability mode for SIC/BK appears in November. The MCA modes for SCE/EUR are not statistically significant, but November shows higher correlation and some statistically significant anomalies preceding the winter NAO. Changes in temperature, specific humidity, SIC/BK and SCE/EUR in November are modulated by an anomalous anticyclonic circulation over the Ural-Siberian region that appears to be a precursor of the winter NAO.

I. INTRODUCTION

The North Atlantic Oscillation (NAO) is one of the most prominent and recurrent patterns of atmospheric circulation variability in the Northern Hemisphere (Hurrel et al. 2003). It can be described as a seesaw of atmospheric pressure in the North Atlantic basin between the Iceland Low and the Azores High. A negative NAO phase exhibits positive anomalies of sea level pressure at high latitudes and negative anomalies over the central North Atlantic, the eastern United States and western Europe (see Fig. 1a). A positive NAO phase yields the opposite pattern. Understanding the processes that potentially trigger the NAO is crucial to improve its predictability. Many recent studies have highlighted the potential predicting role of Arctic sea ice, particularly over the eastern Arctic, and continental snow over Eurasia in autumn, with a reduction of sea ice concentration (SIC) over the Barents-Kara Seas and an increase of snow cover extent (SCE) across Siberia, being followed by a negative NAO phase in the following winter.

Sea ice reduction acts as a source of heat and moisture fluxes that can impact both local and large-scale atmospheric circulation. Observational studies (e.g. García-Serrano 2015; King et al. 2016) and sensitivity experiments with atmospheric general circulation models (AGCMs) (Kim et al. 2014; Nakamura et al. 2015; Sun et al. 2015) have found that an anomalous anticyclone over northern Eurasia related to low SIC over Barents-Kara (SIC/BK) tends to evolve into a negative NAO pattern trough a lagged stratospheric pathway. This mechanism is triggered by the anomalous diabatic heating from the ice-free oceanic areas that can affect the tropospheric circulation. These tropospheric anomalies are associated with a Rossby wave-like anomaly crossing Eurasia that can interact with the climatological wave pattern. If they are in phase (constructive interference), upward propagation of wave activity can reach the stratosphere weakening the polar vortex. The downward response decelerates the westerlies in the North Atlantic sector shifting the storm-tracks southward, which is linked to a negative NAO phase (e.g Hurrell et al. 2003).

Snow variations affect the atmosphere via changes in reflectance of short-wave solar radiation (albedo), emissivity of long-wave radiation, insulation of the atmosphere from the soil below, and latent-heat and water-release in association with melting (e.g. Cohen and Rind 1991). Observational studies (e.g. Cohen et al. 2007; Wegmann et al. 2015) and AGCM experiments (e.g. Peings et al. 2012) show that an increase in the continental SCE over Eurasia (SCE/EUR) also favors a negative NAO phase. The physical mechanism proposed is similar to the one described for Arctic SIC involving a stratospheric pathway. In this case, the onset of the troposphere-stratosphere interaction relies on the regional radiative cooling induced by positive SCE anomalies over central Eurasia, which reinforces the Siberian High. The associated circulation anomalies show a baroclinic structure with height, yielding an anomalous cyclone at the upper troposphere that constructively interfere with the climatological wave pattern.

The linkage between these two potential predictors of the winter NAO, i.e. SIC/BK and SCE/EUR, is still an open question. Gathak et al. (2012) suggest that the sea-ice forcing through changes in moisture fluxes is necessary and sufficient to modulate snowfall in Siberia. The aim of this work is to complement their analysis and to get insight into the relationship between SIC/BK and SCE/EUR in their connection with the winter NAO. The following section describes the methodology and datasets used. Section III describes the results split in three parts: in the first one, we investigate the covariability of SIC/BK and SCE/EUR in late autumn with the winter NAO; in the second one, we explore the contemporaneous anomalies of the atmospheric circulation related to the SIC/BK and SCE/EUR predictors; in the third part, we investigate the regional surface conditions and processes responsible for the potential SIC/BK-SCE/EUR linkage. Finally, in Section IV, we draw the main conclusions and discuss future prospects.

* Electronic address: otinms@gmail.com

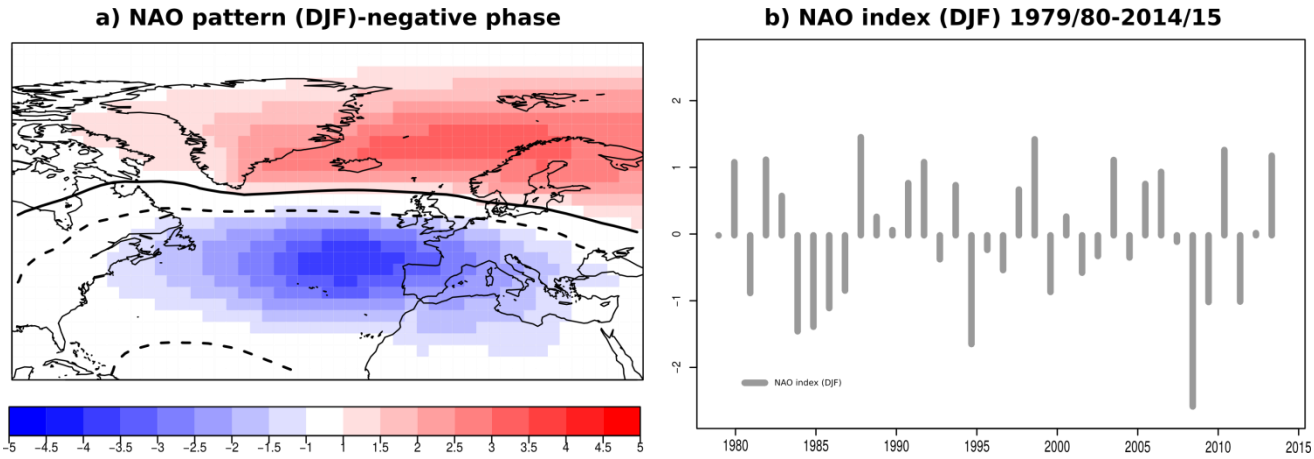

Figure 1. - Left: Leading EOF of detrended sea level pressure anomalies over the North Atlantic-European (NAE) region, with a fraction of explained variance of 51.4 %; note that the negative phase of the NAO is shown. Statistically significant areas at 95% confidence level based on a two-tailed Student's test are contoured. Right: Leading principal component from the EOF analysis of SLP/NAE anomalies, namely the winter NAO index.

II. DATA AND METHODOLOGY

Climate may be seen as a coupled system involving the ocean, the sea-ice and the atmosphere that presents a multivariate and multiple-time probability distribution of states. Developing statistical techniques together with the understanding of dynamical and physical processes are a primary goal of climate research. In this study, empirical orthogonal function (EOF; von Storch and Zwiers 2001) and maximun covariance analysis (MCA; Bretherton et al. 1992) are used to describe the spatial-temporal structure of SIC/BK and SCE/EUR variability as well as the corresponding covariability with winter SLP over 1979/80-2014/15.

The predictor fields are SIC in the eastern Arctic, in particular, over the Barents-Kara Seas (BK: 50ºN-90ºN, 30ºW-120ºE) and Eurasian SCE (EUR: 20ºN-90ºN, 0º-150ºE). We use monthly SIC data from HadISST (Hadley Center Sea Ice and Sea Surface Temperature; Rayner et al. 2003) at 1^{o}x1^{o} resolution. This data-set combines historical ice charts (from shipping, expeditions and other activities), passive microwave satellite acquisitions and NCEP (National Centers for Environmental Prediction) operational ice analyses. We use weekly SCE data from the Global Snow Laboratory at Rutgers University (Robinson et al. 1993), a product derived from the NOAA/NCDC Northern Hemisphere snow cover extent data record and satellite passive microwave brightness temperatures. For SCE, October is defined as the average of the calendar weeks 40-44 (Cohen and Jones 2011), and November of the weeks 44-48. Monthly data of atmospheric variables are given by ERA-Interim reanalysis available from the European Center for Medium-Range Weather Forecasts (ECMWF) at 2.5ºx2.5º resolution. This study focuses on interannual variability rather than on longer-term trends, so to retain variability around the trends all anomalies are detrended before analysis. Different detrending methods, including 1^{st}-order (lineal), 2^{nd}-order (quadratic) and 3^{rd}-order (cubic) polynomial fits, have been evaluated to assess robustness of the results. Unless otherwise stated, the results shown below are based on cubicly detrended anomalies.

EOF analysis consists in decomposing a field into orthogonal basis functions that aims at explaining the maximum amount of variance. The output of the analysis is a set of spatial patterns that are called EOFs and associated standardised time-series called Principal Components (PCs). Thus, the variability of a particular field can be reconstructed by the linear combination of the EOFs and PCs multiplied by their eigenvalues, which represent the fractions of explained variance. The NAO index can be defined as the leading PC corresponding to the leading mode (first EOF) of sea level pressure anomalies in the North-Atlantic-European region (NAE: 20ºN-90ºN, 90ºW-40ºE;e.g. Hurrell et al. 2003) (Figure 1).

In MCA, instead of decomposing a single field, the diagonalization (i.e. singular value decomposition, SVD) is applied to the covariance matrix $(C_{XY})_{MxN}$ of two different fields (X_{MxN}, Y_{LxN}) that are examples of different spatio-temporal structures but that share a common sampling dimension (actual time; N). In this case, the output consists of pairs of spatial patterns each one corresponding to a field (U, V), an associated standardised time-series called expansion coefficients (X^*, Y^*). Each MCA mode is characterized by the squared covariance (sc) (eigenvalue of the covariance matrix Σ), the squared covariance fraction (scf) which is a measure of the fraction of explained covariance compared to other modes, and the correlation between the expansion coefficients (cor).

$$C_{XY} = \frac{1}{N} \cdot X \cdot Y^T \overset{SVD}{\Longrightarrow} C_{XY} = U \cdot \Sigma \cdot V^T$$

$$X^* = U^T \cdot X;$$
$$Y^* = V^T \cdot Y;$$

In this study, MCA is applied considering SIC/BK or SCE/EUR in autumn as predictor fields, and SLP/NAE in winter as predictand field. We only analyse the first MCA mode in each case. To determine statistical significance of these MCA modes, we perform a Monte Carlo test based on 100 permutations shuffling only the atmosphere field (i.e. SLP) with replacement. By performing a MCA upon each

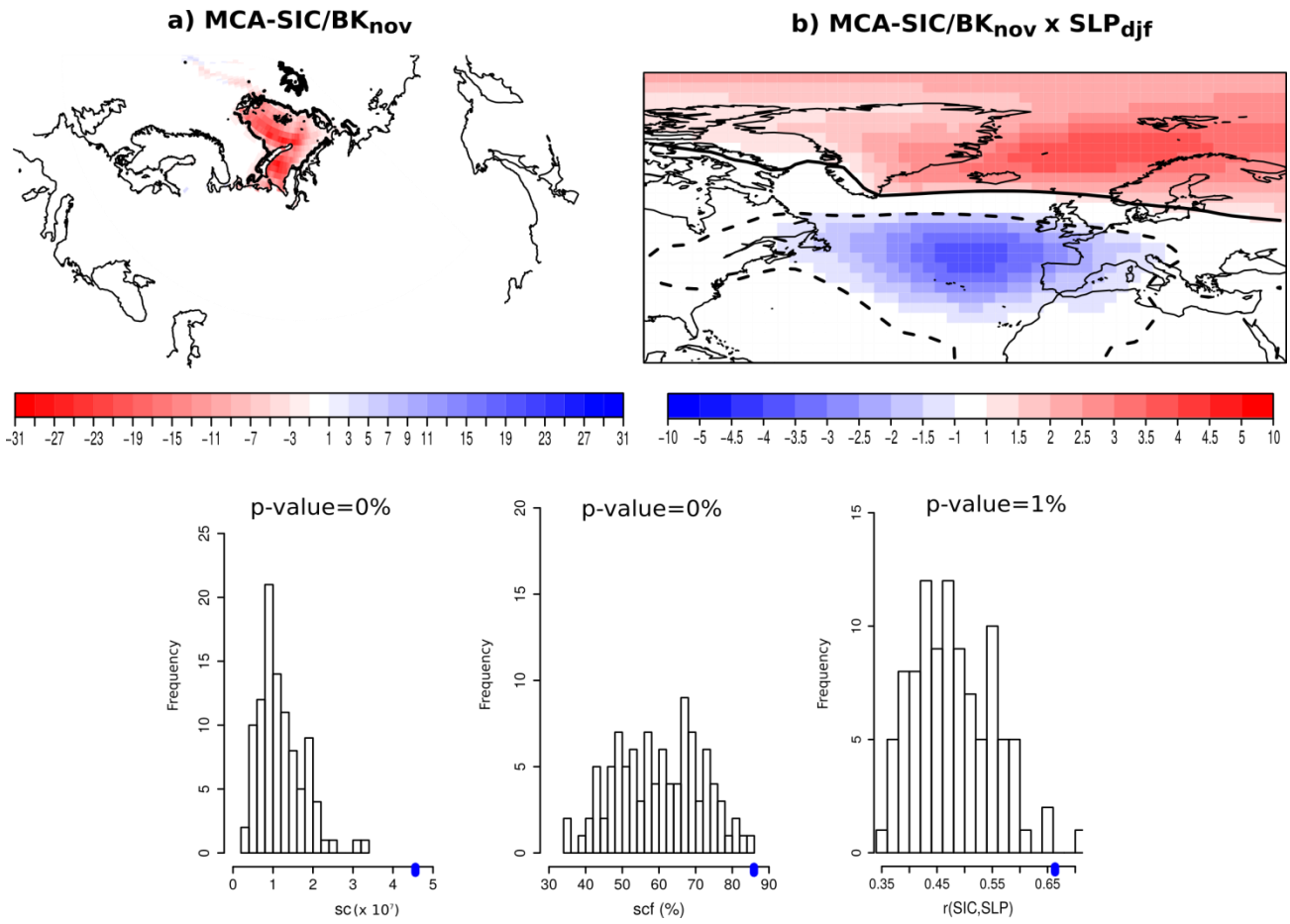

Figure 2.- Top: Leading MCA mode between SIC over Barents-Kara Seas (%; a) in November and winter SLP over the North Atlantic-European region (hPa; b); statistically significant anomalies areas at 95% confidence level based on a two-tailed Student's test are contoured. Bottom: Probability Density Function (PDF) generated in the Monte Carlo test for statistical significance applied to (left) sc=4.5x10^7, (center) scf=85,9%, and (right) cor=0.66 (blue marks), based on 100 permutations shuffling only the atmospheric field (SLP) with replacement.

resampling we generate a probability density function (PDF) that we use to compute the significance level (hereafter simply p-value) which corresponds to the number of randomized values (sc, scf or cor) that exceed the actual value being tested (e.g. García-Serrano et al. 2015).

To explore the dynamics involved in the lagged relationships, regression maps are computed by projecting different anomalous fields onto a time-series, either the NAO index or the MCA expansion coefficients. In this case, the statistical significance of the regressed anomalies is tested with a two-tailed Student's t-test at 95% confidence level.

III. RESULTS

A. Covariability and predictability: SIC/BK and SCE/EUR

The observational lagged influence of the Arctic SIC on the NAO pattern is dominated by sea-ice changes along the Barents-Kara Seas in autumn (García-Serrano et al. 2015) and Greenland-Barents Seas in winter (García-Serrano and Frankignoul 2015). By performing AGCM sensitivity experiments, Sun et al. (2015) found that only SIC changes in the Atlantic sector lead to NAO/AO-like circulation anomalies. Hence, we perform MCA based on SIC anomalies in the Barents-Kara Seas for each autumnal month (September to November) in order to identify which month exhibits the strongest link with the winter NAO.

The leading MCA mode based on September SIC/BK anomalies explains 62% of scf (p-value 27%), with a sc of 1.68x10^7 (p-value 11%) and yields a cor of 0.56 (p-value 20 %). These high p-values indicate a low significance level of this relationship (not shown). For October, the leading MCA mode explains 88% of scf (p-value 0%), with a sc of 6.20x10^7 (p-value 0%), and yields a cor of 0.60 (p-value 2 %) (not shown). The leading MCA mode based on November SIC/BK anomalies explains 86 % of scf (p-value 0%), with a sc sc of 4.56x10^7 (p-value 0%), and yields a cor of 0.66 (p-value 1%) (see bottom row in Figure 2). It appears that MCA-SIC/BK in November exhibits the highest significant correlation with the winter SLP/NAE anomalies which is consistent with previous studies (García-Serrano et al. 2015; Koenigk et al. 2015; King et al. 2015; Yang et al. 2016). Even though MCA-SIC/BK in October is also significant, the dynamics of its influence on the winter atmospheric circulation is not clear (García-Serrano et al. 2015). Thereby, hereafter we focus our analysis on November SIC variability. Figure 2 shows the SIC homogeneous regression map (Fig. 2a) and SLP heterogeneous regression map (Fig. 2b). The SIC pattern shows negative anomalies (i.e. sea-ice retreat) over the northern Barents Sea and over the whole Kara Sea.

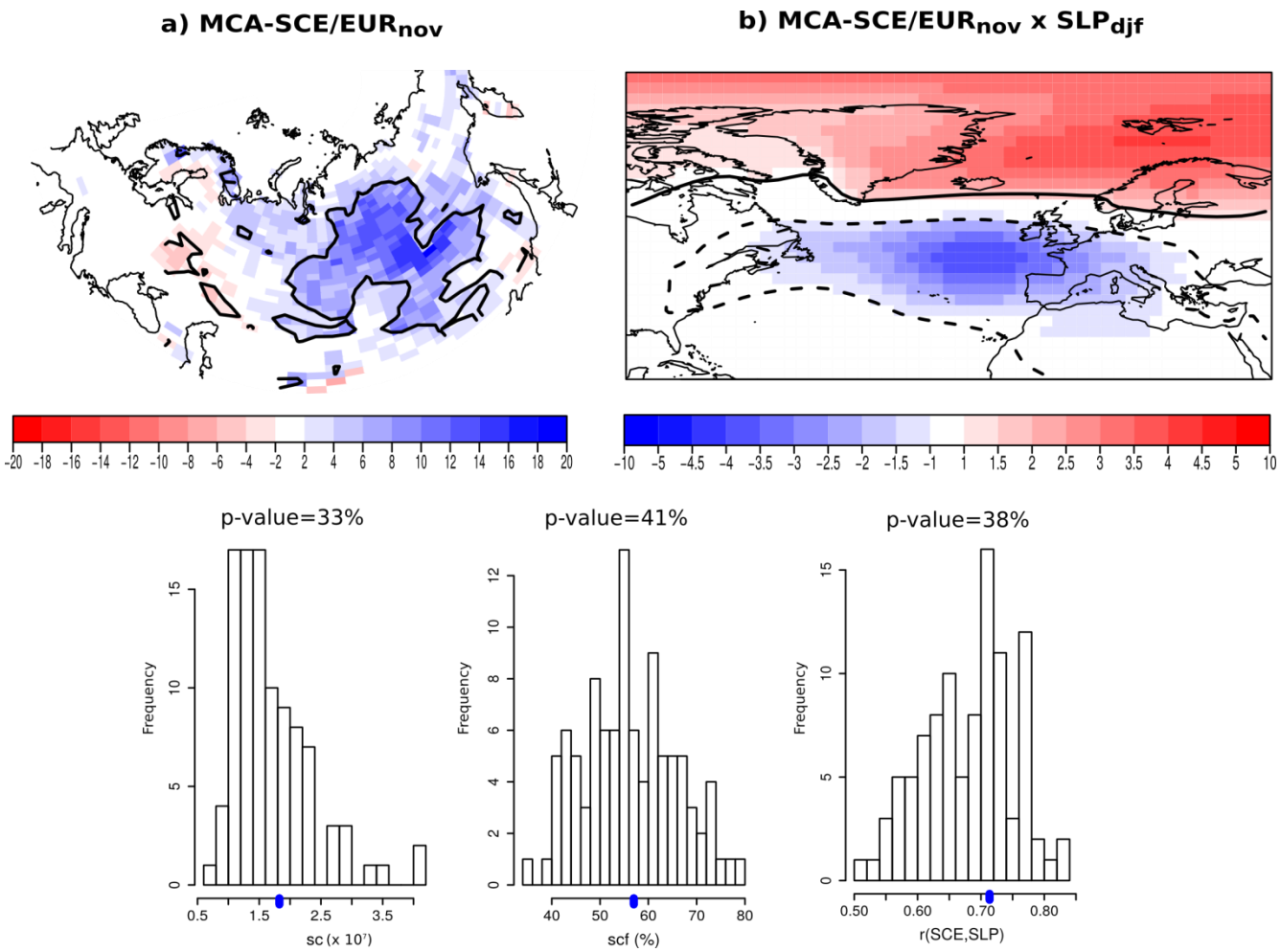

Figure 3.- Top: Leading MCA mode between SCE over Eurasia (%; a) in November and winter SLP over the North Atlantic-European region (hPa; b); statistically significant anomalies areas at 95% confidence level based on a two-tailed Student's test are contoured. Bottom: Probability Density Function (PDF) generated in the Monte Carlo test for statistical significance applied to (left) sc=1.8x10^7, (center) scf=57.0%, and (right) cor=0.71(blue marks), based on 100 permutations shuffling only the atmospheric field (SLP) with replacement.

The SLP pattern strongly resembles the negative phase of the NAO (Fig. 1a). The high confidence levels of the MCA statistics suggest that November SIC/BK anomalies are preferably followed by NAO-like variability in winter.

Caution is required to examine if the modes provided by MCA correspond to intrinsic variability of SLP/NAE and SIC/BK. For that purpose, we compare the MCA expansion coefficients with the principal components of the corresponding EOF analysis. The expansion coefficient MCA-SLP/NAE (DJF) has a correlation of 0.99 with the winter NAO index. Thus, we can argue that the leading covariability mode of winter SLP-NAE is indistinguishable from the winter NAO. The expansion coefficient MCA-SIC/BK$_{nov}$ yields a correlation of 0.98 with the first regional PC of SIC over the Barents-Kara Seas. It also has a high correlation with the first mode of SIC in the Northern Hemisphere (0.93). These results are robust under different detrending methods. Hence, the leading covariability mode of SIC/BK also represents a leading mode of variability in SIC *per se*. It follows that November SIC/BK anomalies can be considered as a potential predictor of the subsequent winter NAO.

As also introduced in Section I, it has been previously suggested that autumnal snow cover anomalies across Eurasia have a remote effect on the subsequent development of winter surface circulation anomalies resembling the NAO (e.g. Cohen et al. 2007; Fletcher et al. 2009; Peings et al. 2012). Analogous to the procedure followed for SCI/BK, MCA based on SCE/EUR anomalies in late autumn (October-November) are performed. The leading MCA mode based on October SCE/EUR anomalies explains 50% of scf (p-value 42%), with a sc of 5.11x10^7 (p-value 57%), and yields a cor of 0.54 (p-value 87 %). For November, the leading MCA explains 57% of scf (p-value 41 %), with and a sc of 1.82x10^7 (p-value 33%) and yields a cor of 0.71 (p-value 38 %) (see bottom row in Fig.3). Extending the period using reanalysis SCE data (instead of satellite-derived products) would not lead to better statistically significant results (Peings et al. 2013).

In contrast to previous studies (e.g. Cohen et al. 2007), we have found that November SCE/EUR anomalies yield the highest correlation with winter SLP/NAE anomalies, rather than October. This finding is supported by the regression maps of autumnal SCE/EUR anomalies onto the winter NAO index, where October does not show significant anomalies

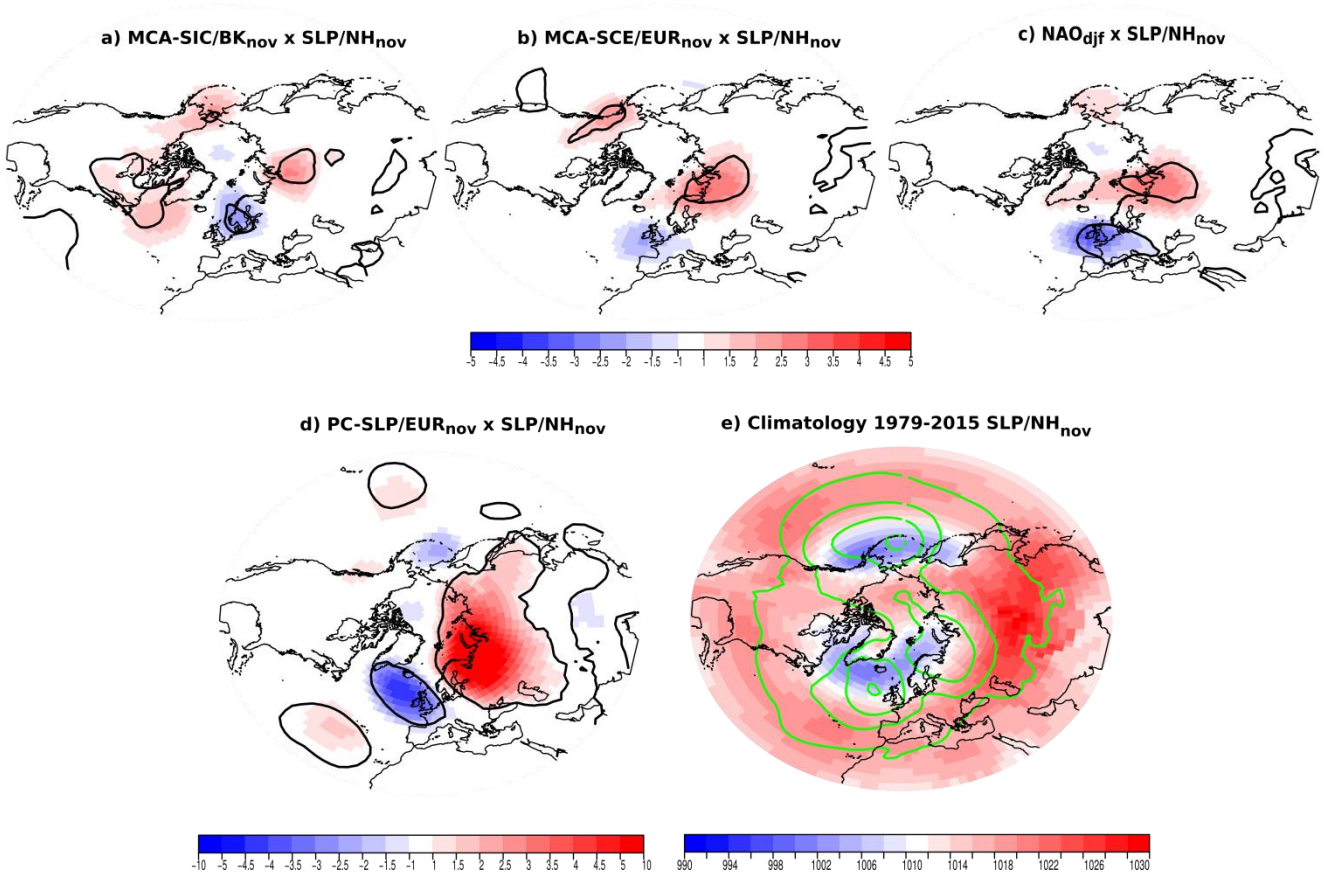

Figure 4.- Regression maps of detrended Northern Hemisphere sea level pressure anomalies onto (a) the MCA-SIC/BKnov expansion coefficient, (b) the MCA-SCE/EURnov expansion coefficient, (c) the winter NAO index, (d) the leading PC from the of the EOF analysis of SLP anomalies over Eurasia (40ºN-90ºN, 0º-150ºN; 41.5% fraction of explained variance). (e) Climatology (hPa; shading) and standard deviation (ci=2hPa; green contours) of SLP in November.

over Eurasia (Fig. A1a) whereas November does so (Fig. A1b). Despite the lack of statistical significance in the MCA-SCE/EUR$_{nov}$ analysis, its high cor (0.71), the NAO-related SCE anomalies in November (Fig. A1b), and results from previous studies (e.g. Cohen et al. 2007; Fletcher et al. 2009; Peings et al. 2012) impede to fully discard November SCE/EUR anomalies as a potential predictor of the subsequent winter NAO. Figure 3 shows the SCE homogeneous regression map (Fig. 3a) and SLP heterogeneous regression map (Fig. 3b) onto the MCA-SCE/EUR$_{nov}$ expansion coefficient. The SCE pattern shows positive and significant anomalies over central Eurasia, while the SLP pattern displays a negative NAO-like signature. Recall that the significance level of this relationship is very low, suggesting that the signal-to-noise ratio is very weak. The associated MCA-SLP/NAE expansion coefficient correlates at 0.99 with the winter NAO index; however, the MCA-SCE/EUR$_{nov}$ expansion coefficient does not correlate well with none of the two leading EOF modes of November SCE/EUR (fvar#1=20%, fvar#2=10 %), with scores below 0.20.

B. Ural-Siberian anticyclone (SCAND)

In order to establish a dynamical framework for the potential influence of November SIC/BK and SCE/EUR on the winter NAO, we investigate the atmospheric circulation anomalies associated with these predictors and those preceding the NAO itself, which could be considered as atmospheric precursors.

Figure 4d shows the regression map of Northern Hemisphere (NH) SLP anomalies in November onto the principal component of the first EOF (EOF1) of SLP in Eurasia (50ºN-90ºN, 0º-150ºE). This regional EOF1 is indistinguishable from the hemispheric EOF1 (r=0.89). This mode exhibits a dipole-like structure with a primary circulation centre over Scandinavia and the Barents-Kara Seas and a weaker centre of opposite sign over western Europe and the North Atlantic basin which can be identified as the Scandinavian pattern (SCAND) a mode of internal variability associated with Rossby wave propagation dynamics and maintained by transient eddy feedback (e.g. Bueh and Nakamura 2007). Interestingly, the centres of action of the SCAND pattern tightly project on the areas of maximum interannual standard deviation (green contours in Fig. 4e). It is thus conceivable that the SCAND pattern represents the dominant mode of November SLP variability in November in both Eurasia and the NH. The statistically significant SLP anomalies preceding the winter NAO also show a dipole-like structure (Fig. 4c), remarkably matching the SCAND pattern. Thus, the results suggest that the November SCAND pattern may evolve into the winter NAO with 1-month lead time, and might be considered as a precursor of the winter NAO (H. Douville et al., in preparation).

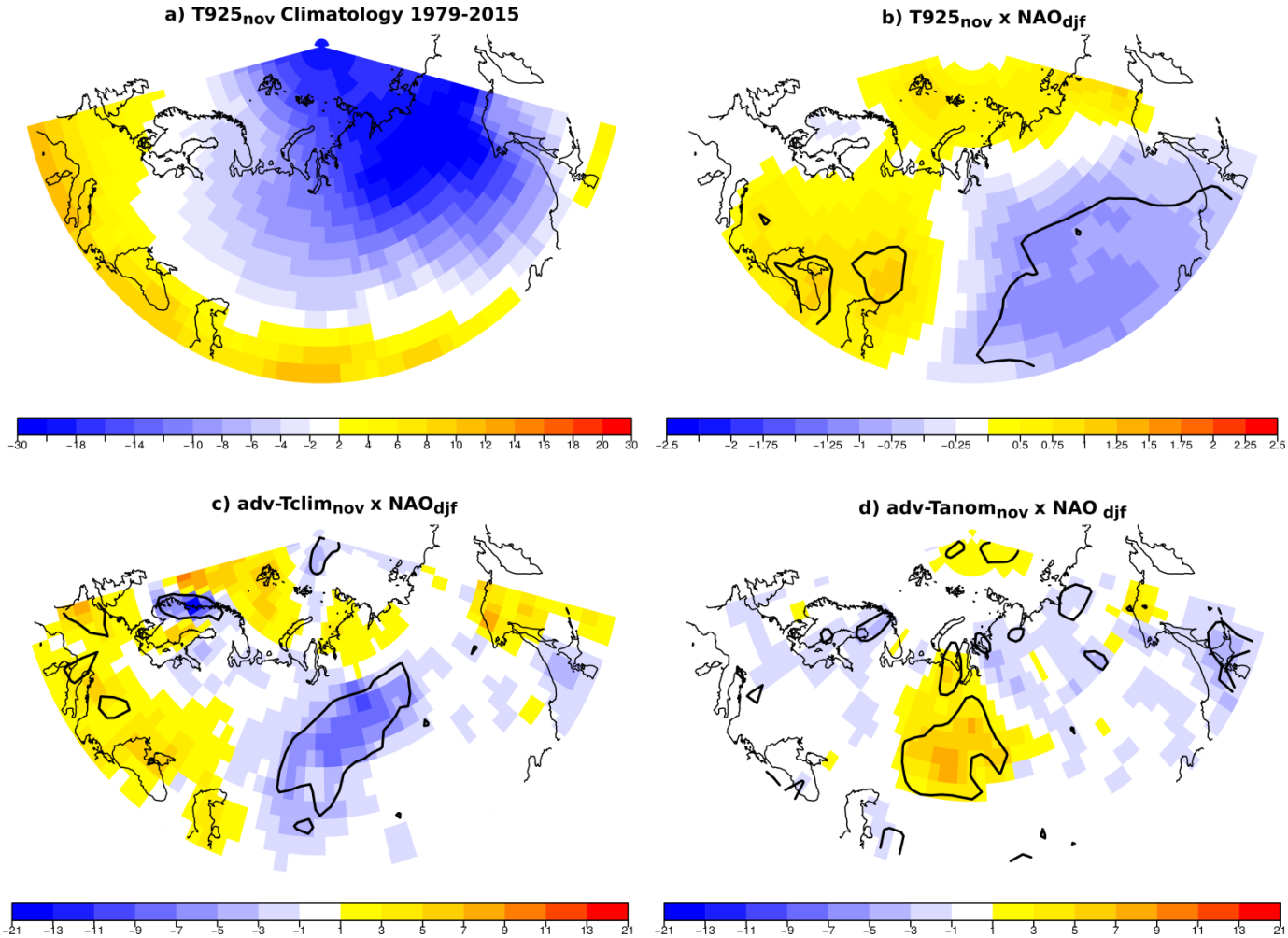

Figure 5.-(a) Climatology of air temperature at 925hPa (T925; ºC) in in November. (b) Regression map of detrended T925 anomalies in November onto the winter NAO index (ºC). (c) Regression map of the advection of climatological T925 by the anomalous flow in November onto the winter NAO index (ºC/s). (d) Regression map of the advection of anomalous T925 by the climatological flow in November onto the winter NAO index (ºC/s).

Figures 4a and 4b show the regression maps of SLP anomalies in November onto the MCA-SIC/BK$_{nov}$ and MCA-SCE/EUR$_{nov}$. The dipole-like pattern associated with SCE/EUR (Fig. 4b) has a strong resemblance to the mode of internal variability (SCAND; Fig. 4d) and to the NAO precursor (Fig. 4c), although only the anomalous anticyclone over the Ural-Siberian region is significant. This suggests that the SCE/EUR anomalies might be driven by the Ural-Siberian anticyclone and not be forcing back the atmospheric circulation, which is also consistent with the lack of statistical significance of the MCA-SCE/EUR (Fig. 3). Also in contrast to previous studies suggesting that the potential SCE influence on the winter NAO is mediated by changes in the Siberian High (e.g. Cohen et al. 2007), our results indicate that the sea level pressure anomaly related to SCE/EUR (i.e. the Ural-Siberian anticyclone) takes place instead over the subpolar low-pressure belt (Fig. 4e).

On the other hand, the dipole-like structure of SLP anomaly associated with SIC/BK (Fig. 4a) is slightly different from the others, as the centres of action are located downstream, with the anticyclonic anomalies shifted toward the continent and the cyclonic anomalies displaced toward the Nordic Seas. We additionally perform a MCA analysis at lag 0 (namely, in November) between SIC/BK and SLP/EUR in order to study whether the atmosphere dominates SIC variability in the Barents-Kara Seas. Note that contemporaneous MCA in mid-high latitudes mainly reflects the atmospheric forcing of the surface field (here SIC), whereas lagged MCA with the surface field leading by more than the atmosphere persistence (~10 days) may reflect the potential feedback onto the atmospheric circulation (e.g. Czaja and Frankignoul 2002). We found that the contemporaneous MCA is not statistically significant (p-values: 22% for sc, 55% for scf, 30% for cor), but the MCA-SLP/EUR pattern projects on the SCAND pattern (Fig. 4d).

This indicates that even being a dominant mode of atmospheric variability in November, the SCAND pattern does not explain much of the SIC/BK variability, which encourages the interpretation of a detectable influence of sea ice variations on the atmosphere (Fig. 4a). The regional reduction of SIC in November may be driven by other mechanism such as the atmosphere in October or the ocean, as proposed by King and García-Serrano 2016. To elucidate the reverse connection, i.e. sea ice influencing SLP anomalies, we recall that model (Honda et al. 2009) and observational (García-Serrano et al. 2015) studies have

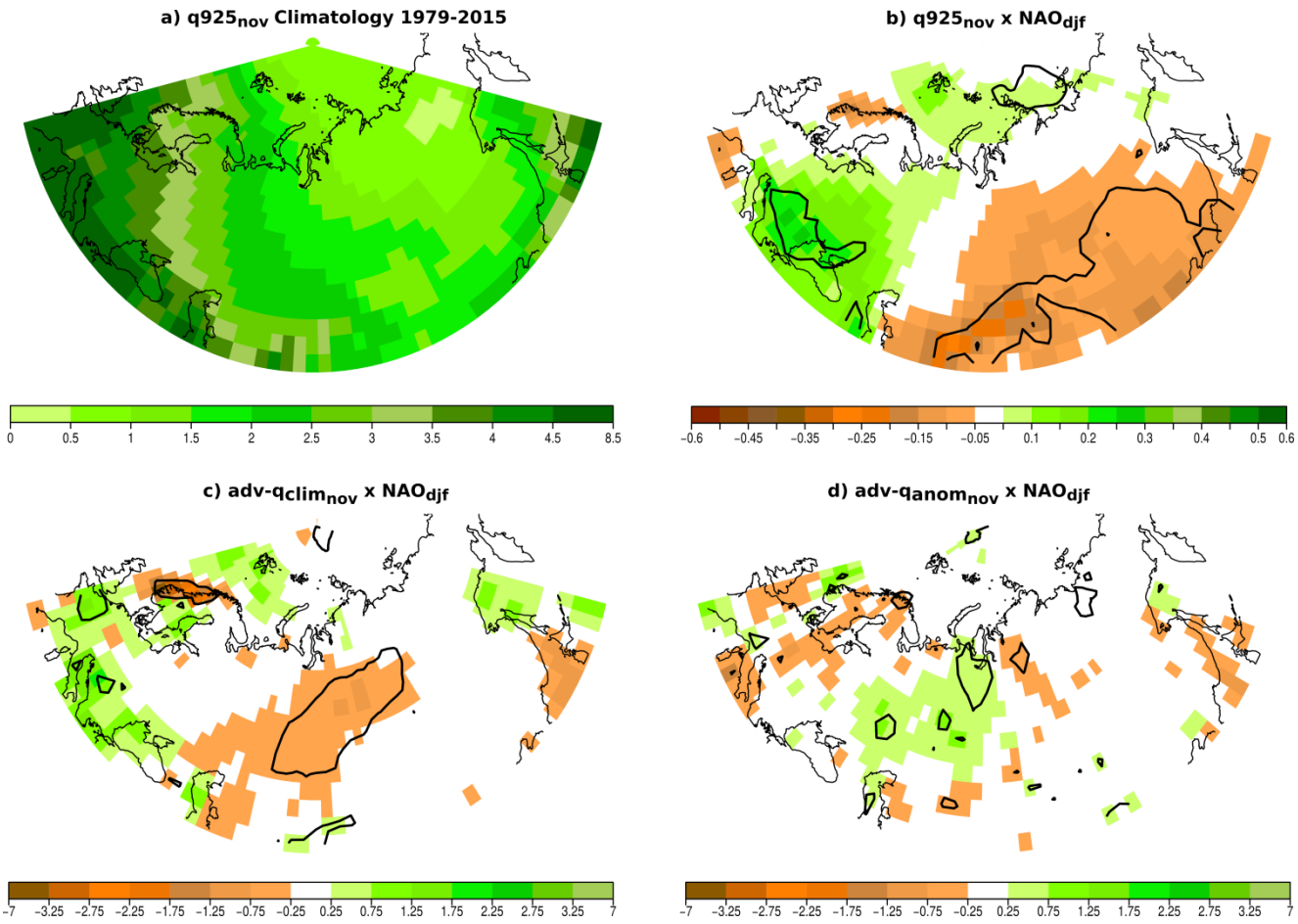

Figure 6.- Same as Figure 5 for specific humidity at 925 (q925; g/kg).

shown a baroclinic structure linked to the Ural-Siberian anticyclone (Fig. 4a). This is speculated to be associated with the large atmospheric variability in the region (Fig. 4e), implying that it is sensitive to surface forcing such as Arctic SIC changes (Santolaria et al., in preparation).

C. Linkage between SIC/BK and SCE/EUR

To explore the relationship between November SIC/BK and SCE/EUR in relation to the winter NAO, we analyse regional surface conditions of temperature and specific humidity in November at 925hPa (40ºN-90ºN, 0º-150ºN) (Figs. 5 and 6, respectively). Climatology in this region shows a cold and dry environment east of Scandinavia (eastern Arctic) and over eastern Eurasia, whereas in western Europe warm and wet conditions prevail (Figs. 5a, 6a). Figures 5b and 6b show regression maps of temperature (T925) and specific humidity (q925) anomalies onto the winter NAO index, respectively: warm and wet anomalies are found over the Barents-Kara Seas linked to the sea-ice reduction while cool and dry conditions extend across Eurasia related to the anomalous increase in snow cover.

Bottom panels in Figures 5-6 display regression maps of the linear advection terms of T925 and q925 onto the winter NAO index: (c) the advection of climatological T925/q925 by the anomalous flow $-v' \cdot \nabla(T_{clim}, q_{clim})$ and (d) the advection of anomalous T925/q925 by the climatological flow $-v_{clim} \cdot \nabla(T', q')$. Note that these anomalous surface conditions in November precede the winter NAO *per se*. Similar anomalies are found using either MCA-SIC/BK_{nov} or MCA-SCE/EUR_{nov} (not shown). Note that the non-linear advection terms are negligible in terms of amplitude (not shown). In Figures 5d and 6d, the advection of anomalous T925/q925 do not yield statistically significant anomalies over the region with positive SCE anomalies (Figs. 3a, A1b), particularly for specific humidity. Positive anomalies over central Eurasia are associated with the warm and wet advection by the climatological flow from the Mediterranean. These warm and wet conditions do not contribute to the NAO-related SCE anomalies. In Figures 5c and 6c, the advection of climatological T925/q925 is dominated by negative anomalies over central Eurasia, which means that the NAO-related wind anomalies (i.e. the Ural-Siberian anticyclone; Fig. 4c) transport cold and dry air from the Arctic to Eurasia. This is indicative of land cooling effect from the advection of climatological temperature and a humidity sink likely associated with the increase in snowfall. This southward transport is consistent with the NAO- related temperature and specific humidity anomalies (Figs. 5b, 6b).

Back to the analysis presented in Section IIIA of the covariability modes of SIC-BK and SCE-EUR in November with SLP-NAE in winter, we finally explore the correlation between both predictors. Whether the advection of anomalous temperature and specific humidity were significant and dominant, the correlation between SIC/BK and SCE/EUR anomalies would be high, and tropospheric circulation anomalies (i.e. the Ural-Siberian anticyclone)

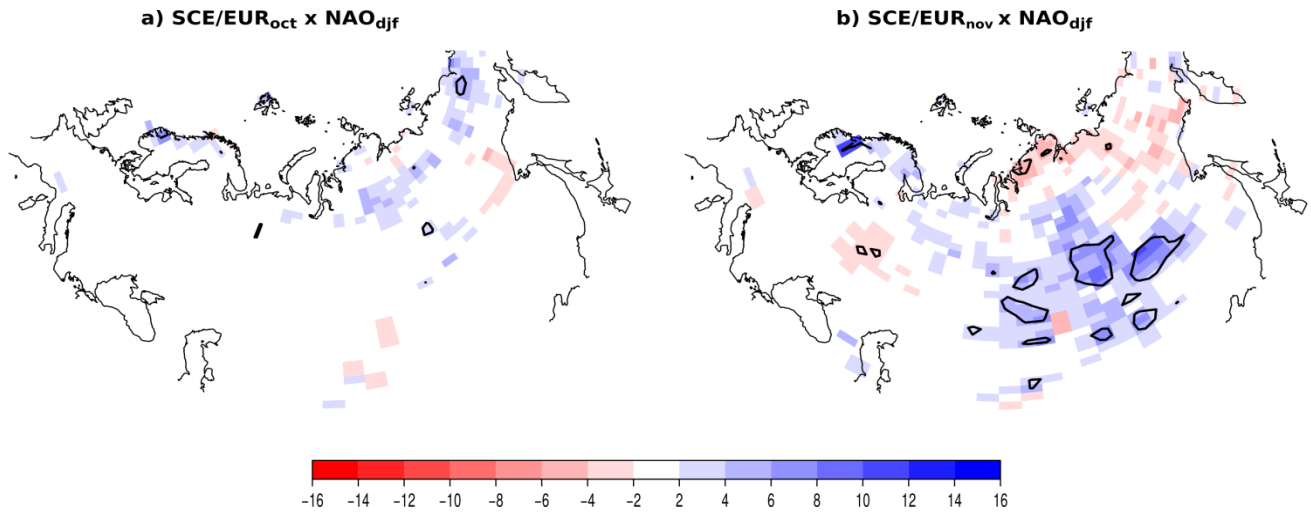

Figure A1.- Regression map of snow cover anomalies in October (left) and November (right) with the principal component of leading mode of sea level pressure anomalies in NAE in winter.

should not play any crucial role in this linkage. However, we found that the expansion coefficients of SIC-BK and SCE/EUR have a correlation of 0.41, which is significant at 95% (>0.35) but not as high as their correlation with the winter NAO (0.66 and 0.71, respectively). It should be recalled that these two covariability modes are constructed by maximizing covariance with the winter NAO. The fact the NAO-related anomalous surface conditions in November are dominated by the advection of climatological temperature and specific humidity may explain why the correlation between both predictors is relatively low, and suggest that the anomalous anticyclonic circulation over the Ural-Siberian region may be the driver linking SIC/BK anomalies with SCE/EUR anomalies.

IV. CONCLUSIONS

The aim of this study is to further explore the influence of interannual variability in autumn Arctic sea ice concentration (SIC) and Eurasian snow cover extent (SCE) on the winter sea level pressure (SLP) in the North Atlantic-European (NAE) sector, as well as to investigate the relationship between both predictors. We have performed maximum covariance analyses (MCAs) over the 1979/80-2014/15 period using SIC over the Barents-Kara Seas on each autumnal month (September to November) and SCE over Eurasia in late autumn (October to November) as predictor fields, with SLP/NAE (DJF) as predictand. The leading covariability mode of September SIC/BK is not statistically significant. For October and November SIC/BK we found significant correlation showing that sea-ice reduction is followed by a negative phase of the winter NAO. Based on previous observational studies assessing empirical prediction skill from SIC/BK (García-Serrano et al. 2015; Koenigk et al. 2015), we consider that November SIC/BK represents the most robust potential predictor, here yielding the highest correlation coefficient (0.66), and whose teleconnection dynamics appear to involve a stratospheric pathway (also King et al. 2016). A result revealed in this study is that the regional covariability mode of November SIC/BK corresponds to the leading EOF of SIC at regional scale (BK) and also at hemispheric scale, i.e. over the whole Arctic. The leading covariability modes of October and November SCE/EUR are not statistically significant, unexpectedly as compared to previous studies using different approaches (e.g. Cohen and Jones 2011; Furtado et al. 2016). For November, however, we found a high correlation (0.71) and statistically significant positive anomalies over central Eurasia preceding the winter NAO, which impede to fully discard November SCE/EUR as a potential predictor.

We investigated the dynamical processes underlying the connection between SIC/BK and SCE/EUR in November by analysing atmospheric circulation and surface climate anomalies in Eurasia. We found that NAO-related sea level pressure anomalies over Urals-Siberia project on the regional leading mode of sea level pressure anomalies which is identified as the Scandinavian pattern. This mode of internal variability is dominant in November and seems to precede the winter NAO. The anomalous anticyclonic circulation over Urals-Siberia appear to be responsible of the link between SIC/BK and SCE/EUR via advection of climatological temperature and specific humidity from the Arctic to Eurasia. This result is consistent with NAO-related surface anomalies; that is, cool and dry conditions over the continent associated with an increase in snowfall, and warm and wet conditions in the eastern Arctic related to sea-ice reduction.

Using a climate model, Ghatak et al. (2012) simulate an increase in snowfall over Siberia only when prescribing the observed evolution of Arctic sea ice and regional sea surface temperature, whereas they do not find any snow signal when using Arctic sea-ice climatology. We suggest a possible explanation for the observational (here presented) and modelling results based on the large variability of SLP/EUR in November: sea-ice reduction in the Barents-Kara Seas induces an anomalous anticyclonic circulation (Honda et al. 2009) that advects climatological cold temperature into Eurasia, increasing snowfall and thus, yielding positives anomalies in snow cover extent.

Further work is needed to elucidate the role of the Ural-Siberian anticyclone as a precursor of the winter NAO and to confirm the driving role of the connection between SIC/BK and SCE/EUR.

V. APPENDIX

1. SCE/EUR anomalies in October and November.

Regression map of SCE/EUR anomalies in October (Fig. A1a) and November (Fig. A1b) onto the winter NAO index. No statistically significant anomalies are found in October, while in November there are some positive anomalies over central Eurasia.

2. Glossary

AGCM= atmospheric general circulation model.
BK= Barents-Kara Seas (50ºN-90ºN, 30ºW-120ºE)
cor=correlation.
EOF= empirical orthogonal function.
EUR= Eurasia (20ºN-90ºN, 0º-150ºE).
MCA= maximum covariance analysis.
NAE=North Atlantic-European (20ºN-90ºN, 90ºW-40ºE)
NAO= North Atlantic Oscillation.
sc= squared covariance.
SCAND= Scandinavian pattern.
scf= squared covariance fraction.
SLP= sea level pressure.

Acknowledgments

I would like to thank Dr. Javier García Serrano for introducing me to the captivating world of climate research, his patience and guidance in writing this project. Thanks also to Dr. Martin Ménégoz for his dedicated time, support and for transmitting his strong passion for science. I acknowledge Francisco J. Doblas-Reyes, director of the Earth Sciences Dept. at Barcelona Supercomputing Center BSC, for the opportunity to work in this institution, and in particular, Virginie Guemas and all the members of the Climate Prediction Group for sharing their work and experience with me. I am especially thankful to Dr. Joan Bech for the first piece of advice that has triggered this whole experience. This internship has been funded by the MINECO RESILIENCE project.

VI. REFERENCES

Bretherton, S. B., C. Smith, and J. M. Wallace, 1992: An intercomparison of methods for finding coupled patterns in climate date. J. Climate, 5, 541-560.

Bueh C., Nakamura H., 2007: Scandinavian pattern and its climatic impact. Q J R Meteorol Soc 133:2117-2131.

Cohen, J., and D. Rind, 1991: The effect of snow cover on the climate. J. Climate, 4, 689-706.

Cohen, J., M. Barlow, P. J. Kushner, and K. Saito, 2007: Stratosphere–troposphere coupling and links with Eurasian land surface variability. J. Climate, 20, 5335–5343.

Cohen, J., and J. Jones, 2011: A new index for more accurate winter predictions. Geophys. Res. Lett., 38.

Cohen, J., and coauthors, 2014: Recent Arctic amplification and extreme mid-latitude weather. Nat. Geosci., 7, 627–637.

Czaja A, Frankignoul C., 2002:Observed impact of Atlantic SST anomalies on the North Atlantic Oscillation. J Clim 15:606-623.

Deser, C., R. Tomas, and S. Peng, 2007: The transient atmospheric circulation response to North Atlantic SST and sea ice anomalies. J. Climate, 20, 4751– 4767.

Deser, C.,R.Tomas, M. A. Alexander, and D. Lawrence, 2010: The seasonal atmospheric response to projected Arctic sea ice loss in the late twenty-first century. J. Climate, 23, 333–351.

Fletcher, C. G., S. C. Hardiman, P. J. Kushner, and J. Cohen, 2009:The dynamical response to snow cover perturbations in a large ensemble of atmospheric GCM integrations. J. Climate, 22,1208–1222.

Furtado, J. C., J. L. Cohen, and E. Tziperman (2016), The combined influences of autumnal snow and sea ice on Northern Hemisphere winters, Geophys. Res. Lett., 43.

García-Serrano, J., Frankignoul, C., Gastineau, G. and de la Camara, A. 2015. On the predictability of the winter Euro-Atlantic climate: lagged influence of autumn Arctic sea ice. J. Clim. 28, 5195#5216.

García-Serrano,J., and C. Frankignoul, 2015: On the feedback of winter NAO-driven sea ice anomalies. Clim.Dyn.

Ghatak, D., C. Deser, A. Frei, G. Gong, A. Phillips, D. A. Robinson, and J. Stroeve (2012), Simulated Siberian snow cover response to observed Arctic sea ice loss, 1979–2008, J. Geophys. Res., 117, D23108.

Honda, M., J. Inoue, and S. Yamane, 2009: Influence of low Arctic sea-ice minima on anomalously cold Eurasian winters. Geophys.Res. Lett., 36, L08707.

Hurrel J. W., Y. Kushnir, G. Ottersen, and M. Visbeck, 2003: An overview of the North Atlantic Oscillation. The North Atlantic Oscillation—Climatic Significance and Environmental Impact, Geophys. Monogr., Vol. 134, Amer. Geophys. Union, 1–36.

Hurrell, J. W., and C. Deser, 2009: North Atlantic climate variability: The role of the North Atlantic Oscillation. J. Mar. Syst., 78, 28–41.

Inoue, J., M. E. Hori, and K. Takaya, 2012: The role of Barents Sea ice in the wintertime cyclone track and emergence of a warm- Arctic cold-Siberian anomaly. J. Climate, 25, 2561–2568.

King, M.P., M. Hell, and N. Keenlyside, 2015: Investigation of the atmospheric mechanisms related to the autumn sea ice and winter circulation link in the Northern Hemisphere. Clim Dyn.

Kim B-M, Son S-W, Min S-K, Jeong J-H, Kim S-J, Zhang X, Shim T, Yoon J-H, 2014: Weakening of the stratospheric polar vortex by Arctic sea-ice loss. Nature Comms 5:4646.

Koenigk T, Caian M, Nikulin G, Schimanke S, 2015: Regional Arctic sea ice variations as predictor for winter climate conditions. Clim Dyn.

Nakamura T, Yamazaki K, Iwamoto K, Honda M, Miyoshi Y, Ogawa Y, Ukita J., 2015: A negative phase shift of the winter AO/NAO due to the recent Arctic sea-ice reduction in late autumn. J Geophys Res -Atm 120.

Peings, Y., D. Saint-Martin, and H. Douville, 2012: A numerical sensitivity study of the influence of Siberian snow on the northern annular mode. J. Climate, 25, 592–607.

Rayner, N. A., D. E. Parker, E. B. Horton, C. K. Folland, L. V. Alexander, D. P. Rowell, E. C. Kent, and A. Kaplan, 2003: Global analyses of sea surface temperature, sea ice, and night marine air temperature since the late nineteenth century. J. Geophys. Res., 108.

von Storch, H., and F. W. Zwiers, 2001: Statistical analysis in climate research. Cambridge Univ. Press, UK.

Peings, Y., E. Brun, V. Mauvais, and H. Douville (2013): How stationary is the relationship between Siberian snow and Arctic Oscillation over the 20th century? Geophys. Res. Lett., 40, 183–188.

Robinson, D. A., K. F. Dewey, and R. R. Heim, 1993: Global snow cover monitoring: an update. Bull. Amer. Meteorol. Soc., 74, 1689-1696.

Sun, L., Deser, C. and Tomas, R. A. 2015. Mechanisms of stratospheric and tropospheric circulation response to projected Arctic sea ice loss. J. Clim. 28, 7824- 7845.

Wegmann M et al 2015: Arctic moisture source for Eurasian snow cover variations in autumn Environ. Res. Lett. 10 054015

Yang, X., Yuan, X. And Ting,M.,2016: Dynamical Link between the Barents-Kara Sea Ice and the Arctic Oscillation. J. Clim. 29, 5103-5122.